BRNO UNIVERSITY OF TECHNOLOGY
VYSOKÉ UČENÍ TECHNICKÉ V BRNĚ

FACULTY OF ELECTRICAL ENGINEERING AND COMMUNICATION
FAKULTA ELEKTROTECHNIKY A KOMUNIKAČNÍCH TECHNOLOGIÍ

DEPARTMENT OF CONTROL AND INSTRUMENTATION
ÚSTAV AUTOMATIZACE A MĚŘICÍ TECHNIKY

MODELING AND CONTROL OF ELECTRIC AND THERMAL FLOWS IN FULLY ELECTRIC VEHICLES
MODELOVÁNÍ A ŘÍZENÍ TOKŮ ELEKTRICKÉ A TEPELNÉ ENERGIE V PLNĚ ELEKTRICKÝCH AUTOMOBILECH

DOCTORAL THESIS STATEMENT
TEZE DISERTAČNÍ PRÁCE

AUTHOR — Ing. Jan Glos
AUTOR PRÁCE

ADVISOR — prof. Ing. Pavel Václavek, Ph.D.
ŠKOLITEL

BRNO 2020

KEYWORDS

fully electric vehicle, FEV, automotive, thermal model, thermal flows control, heat pump control, vapor compression refrigeration system control, VCRS, electronic expansion valve, EXV, vehicle thermal management system, VTMS, hybrid model predictive control, HMPC, non-linear model predictive control, NMPC, air quality control, virtual sensors, thermal energy storage, TES

KLÍČOVÁ SLOVA

plně elektrický automobil, tepelný model, řízení tepelných toků, řízení tepelného čerpadla, řízení chladicích systémů, elektronické expanzní ventily, tepelný management vozidla, hybridní prediktivní řízení, nelineární prediktivní řízení, řízení kvality vzduchu, virtuální snímače, zásobník tepelné energie

GLOS, Jan. *Modeling and Control of Electric and Thermal Flows in Fully Electric Vehicles*. Brno, 2020, 36 p. Doctoral Thesis Statement. Brno University of Technology, Faculty of Electrical Engineering and Communication, Department of Control and Instrumentation. Advised by prof. Ing. Pavel Václavek, Ph.D.

Contents

Introduction

Fully electric vehicles (FEV) require special approaches for cabin heating, as the classical solution adapted from an internal combustion engine (ICE) vehicles is not satisfactory from the perspective of energy consumption. ICE vehicles utilize waste heat from the ICE for cabin heating. The ICE's tank-to-wheel efficiency is usually 20 % to 30 %, and approximately 30 % of total energy can be used for cabin heating [1, 2]. If we consider petrol ICE, the energy density is $34.2\,\mathrm{MJ\,l^{-1}}$. For city driving with an average speed of $40\,\mathrm{km\,h^{-1}}$ and average fuel consumption of 8 l/100km, there is an available thermal flow of 9 kW on average for cabin heating.

On the other hand, the electric vehicle (EV) powertrain has a much higher overall efficiency (67 % to 82 %), with approx. 10 % to 25 % converted to waste heat [3]. As a result, the EV generates a maximum waste heat flow rate of approx. 0.85 kW to 2 kW under the same conditions as for the ICE vehicle above. Since the batteries temperature can not exceed approx. 30 °C to 40 °C, the waste heat recovery makes sense in combination with the use of a heat pump system, which would elevate the temperature for cabin heating. Thermal energy storage (TES) could be also used to support heating and cooling.

Regardless of the heat source, a cabin heating system needs to be powered from batteries and the power consumption negatively influences the mileage of the EV. An extremely unpleasant choice can occur when the user needs to decide if the EV will heat the cabin or reach its destination.

This thesis provides innovative control techniques of energetic flows within a fully electric vehicle based on an integrated and systematic approach. The core of that approach is an algorithm called Model Predictive Thermal Decision Controller, which is proposed for decision-making tasks (i.e. transfer heat from here to there). This core algorithm is complemented with the Non-linear Model Predictive Control algorithm for cabin comfort (combined temperature with air quality), which minimizes the thermal losses caused by vehicle cabin ventilation. The third important part deals with model-based vapor compression refrigeration system control, as this system is the backbone of the whole vehicle thermal management system. These leading topics are completed by other supportive components (dynamic models, virtual sensors, graphical user interface, etc.).

1 State-of-the-Art

This chapter describes the current State-of-the-Art (SOA) of relevant parts of the Vehicle Thermal Management System (VTMS) for a passenger vehicle. A disadvantage of today's fully electric vehicles (FEV) is the weather-dependent range, which means that under cold ambient temperatures the range of vehicles dramatically decreases [4] down to less than half of their nominal range. This issue partially depends on increased high-voltage (HV) battery internal resistance under cold conditions [5]. Secondly, this issue is caused also by Heating, Ventilation and Air Conditioning (HVAC) system, which needs to be powered from HV battery. Especially the cabin heating can decrease the vehicle range by $\sim$20 % at an ambient temperature of $-7\,^{\circ}\mathrm{C}$ [6] and even worse for lower temperatures.

A Mercedes-Benz B-class (W242.890) vehicle was used as an SOA example. This car is a fully electric vehicle (FEV) based on the internal combustion engine (ICE) platform.

A comprehensive overview of different possible VTMS approaches for EVs can be found for example in [7].

1.1 Vehicle thermal management system

In FEV High-Voltage Battery temperature needs to be controlled and Electric Motor (EM) with Power Electronics (PE) needs to be cooled. Moreover, the amount of power-train waste heat is quite low, thus it is not sufficient to use only the power-train waste heat for cabin heating and separate heater needs to be used.
The FEV VTMS layout (shown in Fig. 1.1) brings some issues:

- FEV mileage decrease under cold ambient conditions
- High dependency of FEV range on HVAC (especially if cabin heating is active)
- A high number of VTMS components (heat exchangers, pumps, etc.)

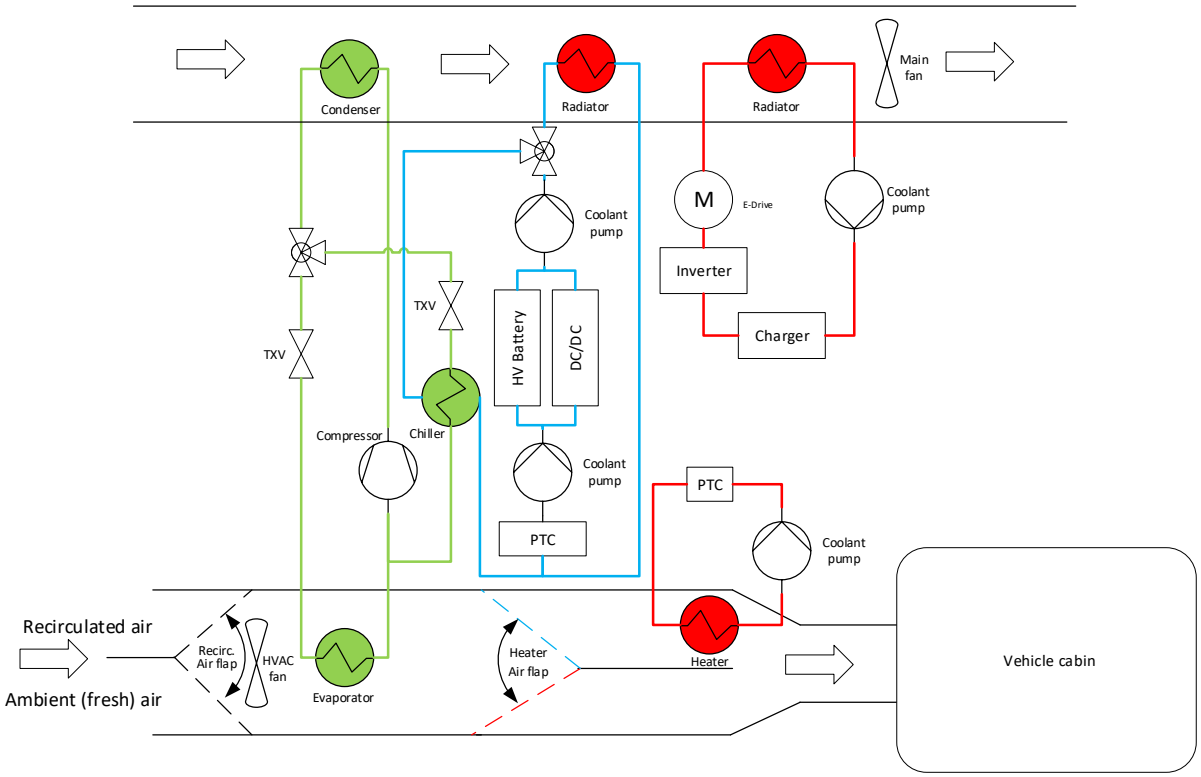

Fig. 1.1: Example of VTMS for fully electric vehicle

1.2 VCRS control

Considering the VCRS system, there are two main configurations possible, a system with a high-pressure receiver complemented by evaporator superheat control and a system with a low-pressure accumulator with a fixed orifice.

The SOA for EXV control is the application of a PI or PID controller for superheat control [8]. The PID control, fuzzy control, and artificial neural network control were implemented for superheat control in [9]. There are also applications of Model Predictive Control (MPC) for VCRS control [10, 11, 12, 13]. A more exhaustive overview of possible approaches can be found in [14].

The FEV SOA example (B-Class) employs electric compressor, condenser and two sets of an evaporator, thermal expansion valve (TXV) and shut-off valve (SOV) (one set for air cooling, the second one for HV Battery cooling).

FEV (B-class) VCRS includes a liquid receiver and it is operated as superheat controlled (the TXV meters the refrigerant flow rate to the evaporator to keep the defined refrigerant superheat degree at evaporator outlet and compressor suction).

2 Goals

The goals of this thesis were partially formulated by the OSEM-EV project proposal and the rest of them appeared during the project solution. In general, this work should give a set of novel modeling and control approaches related to electric vehicle (EV) thermal management.

The basic and general goal of the OSEM-EV project was an increase of the FEV range, especially under adverse ambient conditions (cold winter or very hot summer). Fulfillment of this goal requires the cooperation of different FEV subsystems, e.g. energy-efficient powertrain and batteries, HVAC system, overall thermal management system with low heat losses, etc. The optimality can be only achieved if the subsystems are properly designed, realized and then controlled.

The main goal of this thesis was the research and development of control algorithms ensuring energy-efficient FEV operation. These algorithms can be divided into several groups:

- Low-level control algorithms (compressor motor control, flaps control, fan speed control, etc.)
- High-level control algorithms (HVAC control, VCRS control, HvBat and E-Drive temperature control, etc.)
- Vehicle energy flow routing (Thermal Decision Controller)

2.1 Vehicle thermal management system

A completely new FEV VTMS layout (shown in Fig. 2.1) was designed by AVL List to improve vehicle efficiency.

This layout enables E-Drive and HV Battery waste heat recovery, cabin heating by VCRS and also incorporates thermal energy storage (TES). The designed VTMS is a little bit more complicated (from circuit and valves perspective), but it also saves some components (fewer pumps and heat exchangers).

The goal was to complete the proposed VTMS with suitable control algorithms for both the simulations and real operation. The algorithms should assure compliance of constraints (like HV Battery and ED temperature range,

etc.) and also regulation to defined references (cabin temperature).

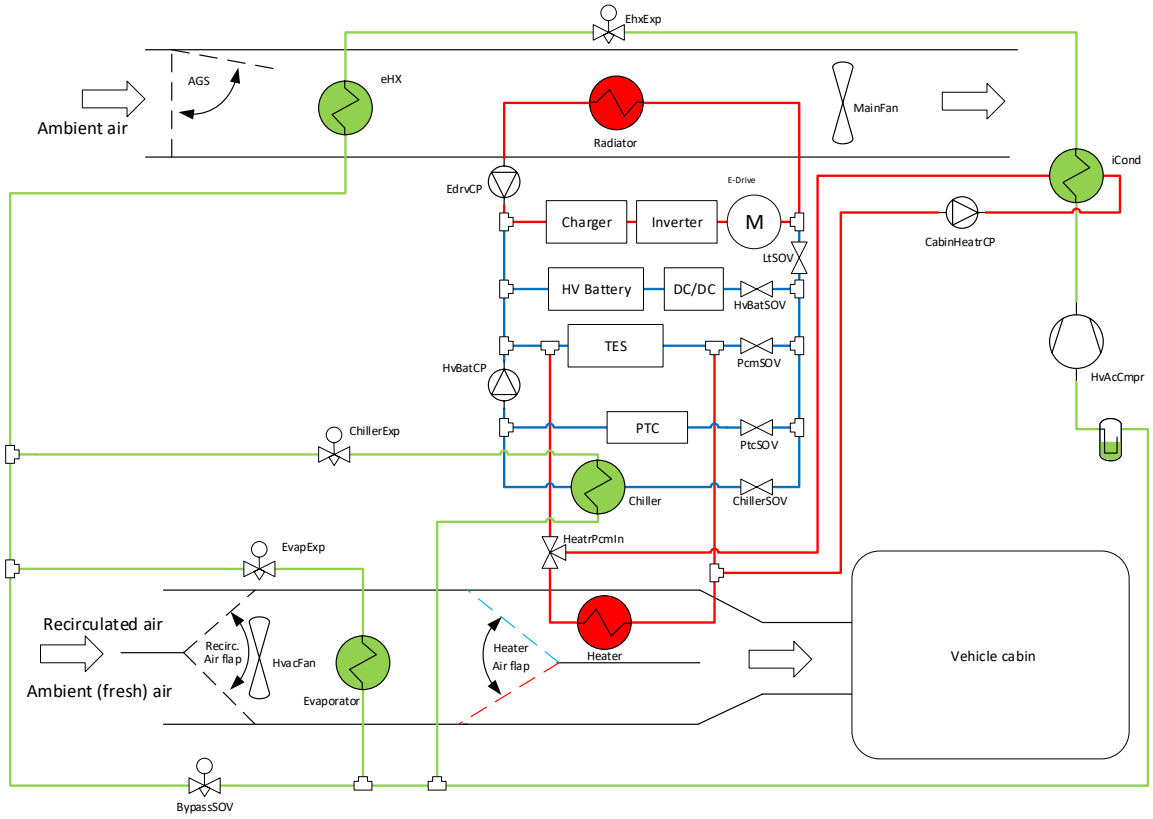

Fig. 2.1: VTMS for a fully electric vehicle from OSEM-EV project

2.2 VCRS control

The OSEM-EV proposed solution includes a suction line accumulator, which ensures pure vapor (no liquid) refrigerant at compressor suction and also serves as a refrigerant reservoir. The EXVs are used to control the condenser subcooling to achieve the best performance of the VCRS.

It was found in [15] that condenser subcooling (SC) has a significant influence on the Coefficient of Performance (COP) and several methods of optimal SC determination were introduced in [16, 17, 18].

In contrast to SOA VCRS control, the OSEM-EV VCRS circuit requires a much more sophisticated control approach and also allows system efficiency improvement. The goal was to design the control algorithms concerning all possible operating modes, e.g. heating and cooling with different heat sources and sinks configuration.

3 Control of electro-thermal flows

Control algorithms were prepared for whole the VTMS shown in Fig. 2.1. The control algorithms are organized into three sets (MATLAB/Simulink models), each of them representing HVAC, HV Battery, and ED control algorithms. These sets of algorithms are based on PI controllers, so the detailed description is omitted as these approaches are generally known. For selected parts of VTMS, innovative algorithms were designed and their description is included within this chapter.

The algorithms (both the basic and advanced) were tested on the overall Dymola model and also they were partially tested on the assembled test bench.

3.1 VCRS model-based EXV control

Compressor speed (and thus cooling/heating power) can be quite easily controlled, but EXV control is much more tricky - in Vapor Compression Refrigeration System (VCRS) with suction accumulator the EXV should ensure defined condenser subcooling (e.g. 5..10 K; representing optimal COP). Issues of a simple PI controller approach are:

1. Reduced VCRS performance during startup
2. Subcooling (SC) measurement definition area ($SC > 0$)

The solution of problems above was found in the form of model-based feedforward EXV control, which is described within the following text.

3.1.1 EXV refrigerant mass flow rate computation

Using equation

$$\dot{m}_{\mathrm{cmp}} = \frac{\omega}{2\pi}\rho V \eta_{\mathrm{vol}}, \tag{3.1}$$

we can compute the expected refrigerant mass flow rate of the compressor and by employing

$$\dot{m}_{\mathrm{xv}} = C_{\mathrm{d}} A \sqrt{2\rho\,(p_{\mathrm{i}} - p_{\mathrm{o}})}. \tag{3.2}$$

we can get the mass flow rate through the EXV.

In steady-state we suppose that these refrigerant mass flow rates are equal $\dot{m}_{\mathrm{xv}} = \dot{m}_{\mathrm{cmp}}$ and by combining (3.2) and (3.1) and by some reordering we can get an equation for estimated EXV effective area needed for steady-state VCRS operation under usual conditions

$$A = \frac{\frac{\omega}{2\pi}\rho_{\mathrm{sv}}(p_{\mathrm{e}})V_{\mathrm{cmp}}\eta_{\mathrm{vol}}}{C_{\mathrm{d}}\sqrt{2\rho_{\mathrm{sl}}(p_{\mathrm{c}})\,(p_{\mathrm{c}} - p_{\mathrm{e}})}}. \tag{3.3}$$

An additional PI controller was proposed to ensure disturbance rejection and to control the subcooling to optimal reference value with no steady-state error as shown in Fig. 3.1. This approach of EXV control was implemented into Thermo-Electric Management Control Unit (TEMCU) and evaluated on the test bench with results presented in Fig. 3.2. It is evident that this control approach gives great results in terms of subcooling reference tracking and substantially improves the VCRS system startup. The subcooling reference is tracked without any significant control error and the system is capable to cool the air immediately after the compressor startup.

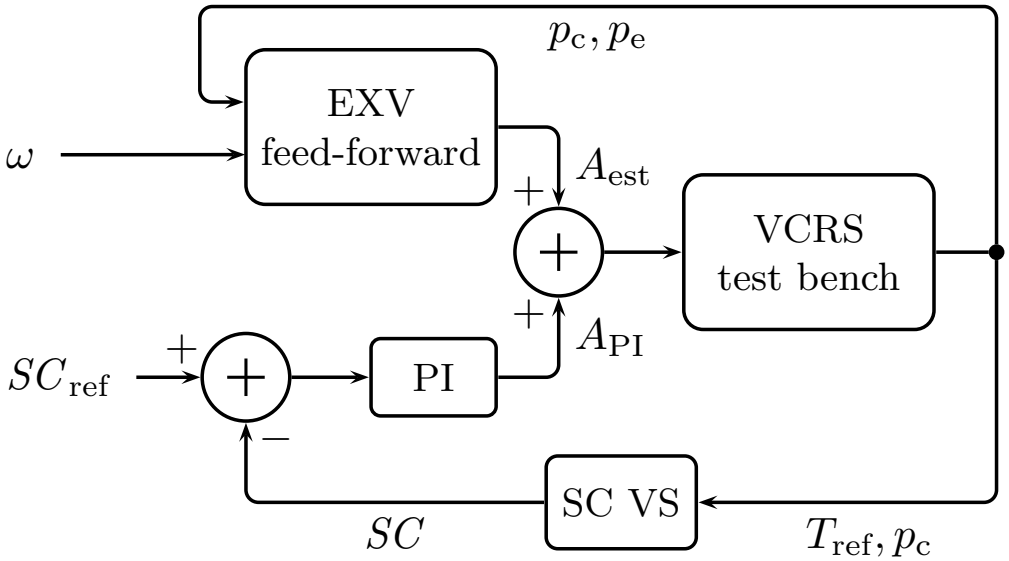

Fig. 3.1: Model-based VCRS EXV control loops.

The presented method of EXV SC control could be (with minor changes) also applied to VCRS EXV superheat control.

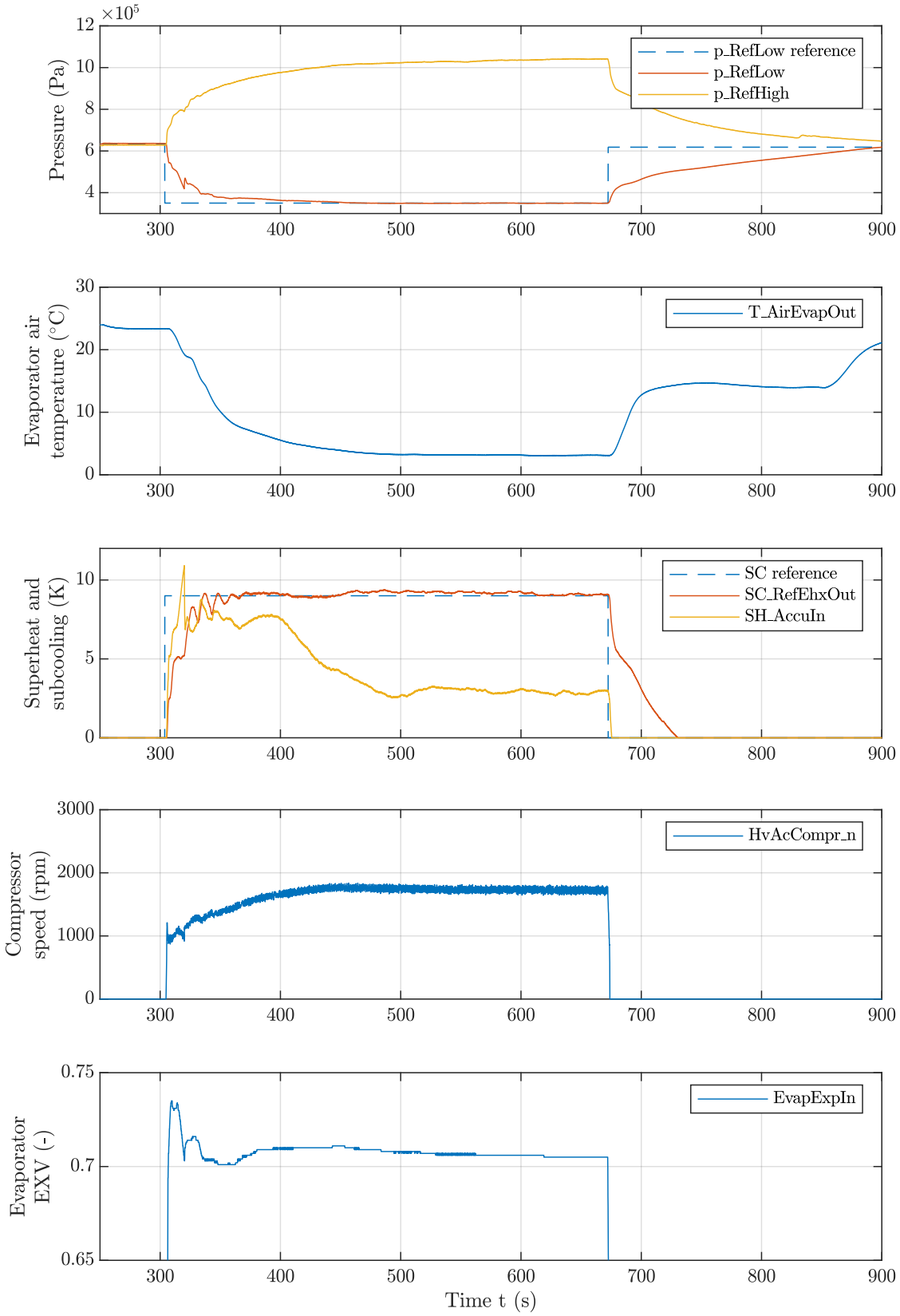

Fig. 3.2: Test bench measurements of model-based EXV control

3.2 Cabin temperature control

This section aims to design energy-efficient control of cabin air temperature. Vehicle cabin needs to be ventilated, but the exhausted air carries out heated or conditioned air, which leads to substantial energy losses. As this issue is more significant in winter during cabin heating, we will consider this case. The summer operation would be very similar when considering cooling efficiency.

It is obvious that with full cabin air recirculation, minimal heat requirements would be achieved. Nevertheless, this approach can not be used, as no fresh air will be supplied to the cabin and thus the air quality will be deteriorated in terms of a higher carbon dioxide (CO_2) concentration. High concentrations of CO_2 can lead to driver (and also passenger) fatigue [19].

As a first preview of the required thermal flows for vehicle cabin heating, we performed a set of simulations, whose results are presented in Fig. 3.3. Both the required heat and the resulting cabin air quality are strongly dependent on the fresh air flap setting. Then, two important conclusions can be obtained from Fig. 3.3:

1. The fresh air flap - needs to be kept above approx. 25 % to achieve satisfactory cabin air quality (considering 2 passengers and HVAC fan air mass flow rate $\dot{m}_c = 0.07\,\mathrm{kg\,s^{-1}}$; with possible short-term lower values of the fresh air ratio)
2. A heat source in the order of kW (e.g. 4..8 kW) is needed for cabin heat build-up (note: even all the waste heat from an EV powertrain is not sufficient).

Regarding the influence of cabin heating on vehicle range, in the worst-case, the heat source would consume approx. 2.3 kW h per cabin heat build-up and 3 kW h per each hour of driving, with a higher air mass flow rate the power consumption would be also higher. For a mid-size EV (such as a Mercedes-Benz B-class, Nissan Leaf) that means a loss of mileage by 7.6 % due to cabin heat build-up and 10 % per each hour of operation.

At this point, we should summarize the requirements on cabin environment control:

1. Temperature - keep it at a (user) defined reference
2. Air quality - keep it at a reasonable value (approx. 600..1000 ppm, short time up to 1500 ppm)

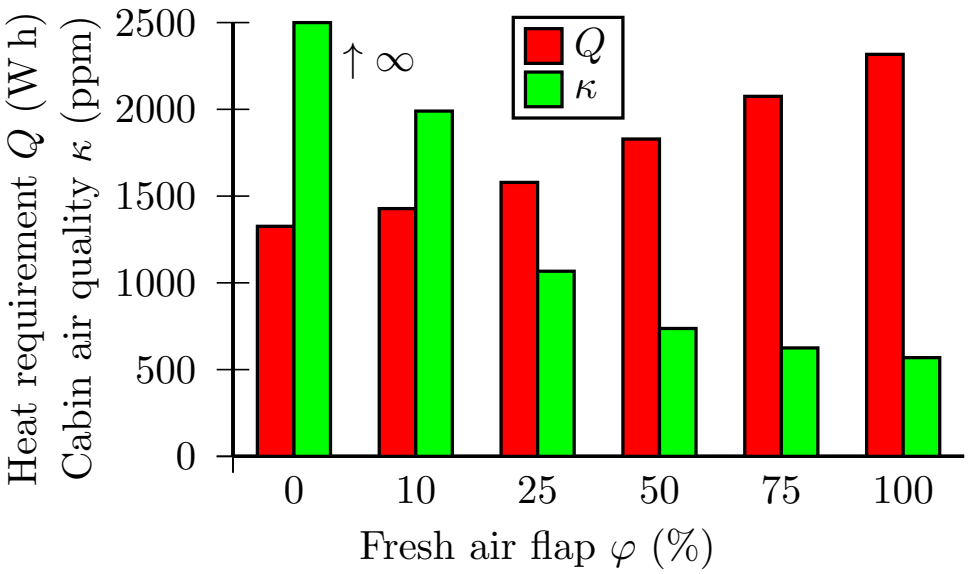

Fig. 3.3: Heat required by a heating system for cabin heat build-up during a 30-minute drive

3. Power consumption - minimize the power of the heat source, fan, and coolant pump
4. Noise - keep the fan speed as low as possible

The controlled system's manipulated variables are constrained, moreover, its internal states and outputs are constrained too (e.g. supply air temperature should not exceed 60 °C, coolant temperature 90 °C, etc.). Considering the above requirements, one of the preferable control approaches is Non-linear Model Predictive Control (NMPC).

The dynamic model of the FEV cabin and HVAC was prepared as a combination of the models described within the doctoral thesis

$$\dot{\mathbf{x}} = \mathbf{f}(\mathbf{x}, \mathbf{u}), \tag{3.4}$$

$$\mathbf{z} = \mathbf{h}(\mathbf{x}), \tag{3.5}$$

with state ($\mathbf{x}$), input ($\mathbf{u}$) and output ($\mathbf{z}$) vectors

$$\mathbf{x} = \begin{bmatrix} T_{\mathrm{c1}} & T_{\mathrm{c2}} & T_{\mathrm{c3}} & T_{\mathrm{c4}} & T_{\mathrm{h1}} & T_{\mathrm{h3}} & T_{\mathrm{h4}} & \kappa \end{bmatrix}^{\mathsf{T}}, \tag{3.6}$$

$$\mathbf{u} = \begin{bmatrix} \dot{m}_{\mathrm{h5}} & \dot{m}_{\mathrm{c}} & \dot{Q}_{\mathrm{h10}} & \varphi \end{bmatrix}^{\mathsf{T}}, \tag{3.7}$$

$$\mathbf{z} = \begin{bmatrix} z_{T_{\mathrm{c1}}} & z_{T_{\mathrm{h1}}} & z_{T_{\mathrm{h4}}} & z_{\kappa} \end{bmatrix}^{\mathsf{T}}, \tag{3.8}$$

$\mathbf{f}(\cdot)$ stands for the right-hand sides of the cabin and HVAC model state equations and $\mathbf{h}(\cdot)$ is a vector of the output functions.

3.2.1 NMPC problem formulation

At each time step of the NMPC algorithm, an optimal control problem (OCP) needs to be solved [20]

$$\min J_N(\mathbf{x_0}, \mathbf{u}(\cdot)) = \sum_{k=0}^{N-1} \|\mathbf{l}(\mathbf{x}_k, \mathbf{u}_k) - \mathbf{r}_k\|^2_{\mathbf{Q}} + \|\mathbf{l}_N(\mathbf{x}_N) - \mathbf{r}_N\|^2_{\mathbf{Q}_N}, \tag{3.9}$$

subject to

$$\mathbf{x}_0 = \hat{\mathbf{x}}_0, \tag{3.10}$$

$$\mathbf{x}_{k+1} = \mathbf{f}(\mathbf{x}_k, \mathbf{u}_k), \tag{3.11}$$

$$\mathbf{x}_k^{\text{lo}} \leq \mathbf{x}_k \leq \mathbf{x}_k^{\text{up}}, \tag{3.12}$$

$$\mathbf{u}_k^{\text{lo}} \leq \mathbf{u}_k \leq \mathbf{u}_k^{\text{up}}, \tag{3.13}$$

where $\mathbf{l}(\cdot)$ and $\mathbf{l}_N(\cdot)$ are vectors of penalized variables, $\mathbf{r}_k$ and $\mathbf{r}_N$ stand for time-varying and final references, $\mathbf{Q}$ and $\mathbf{Q}_N$ are weighting matrices. Then $\mathbf{x}$ denotes the discrete states, $\mathbf{u}$ the control input. Both the states and control inputs can be constrained by (3.12) and (3.13).

3.2.2 Simulations

The simulations described in this section were realized in the MATLAB/ Simulink environment.

The cabin and HVAC model (described in the doctoral thesis) was exported from Dymola into the Functional Mockup Unit (FMU) exchange format and then imported into Simulink using the `FMUtoolbox` [29], a self-developed FMU importing tool for MATLAB/Simulink.

The NMPC controller was gradually tuned using Model in the loop (MIL) and Software in the loop (SIL) simulations and the results are shown for Processor in the loop (PIL) simulation.

The NMPC algorithms were successfully implemented on an Infineon AURIX Tricore TC299TF microcontroller unit (MCU), placed on the AURIX

Starter Kit TC299. The MCU contains three cores running at 300 MHz, 8 MB FLASH (4x2 MB) and 728 kB RAM.

In Fig. 3.4, there is a diagram of the Processor in the Loop (PIL) simulation. The references (**r**) and measured outputs (**z**) from the Dymola model (running under MATLAB/Simulink) are sent to the MCU via TCP/IP communication, and the controls (**u**) are sent from the MCU to the MATLAB Simulink and applied to the Dymola model. The block EKF stands for Extended Kalman Filter, which provides state variables estimations needed by the NMPC algorithm.

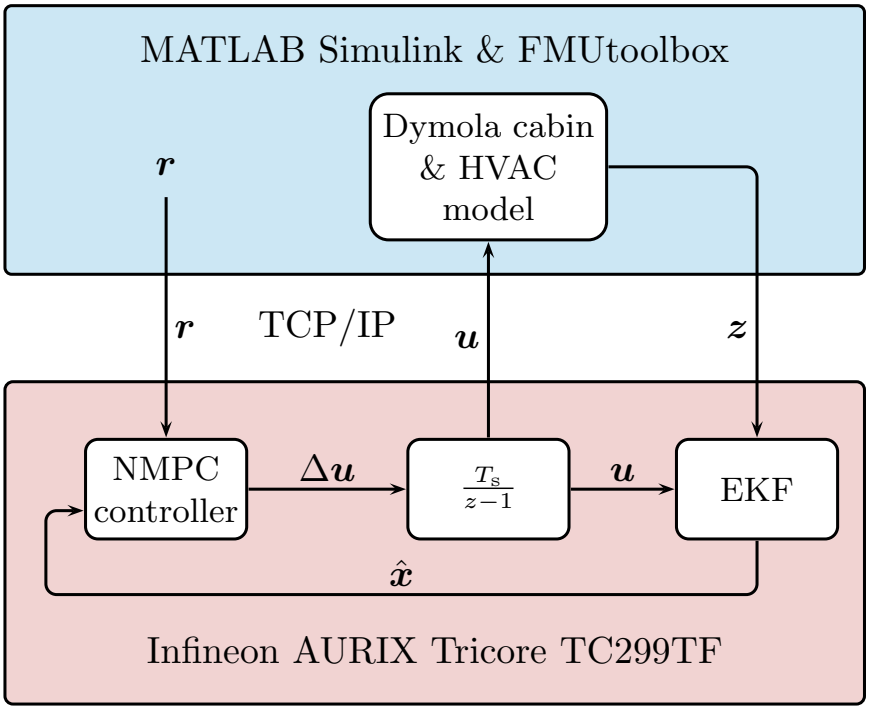

Fig. 3.4: NMPC PIL simulation diagram

In Fig. 3.5 there are results of a simulation of FEV cabin heat build-up under winter conditions. The cabin temperature reference ($r_{T_{c1}} = 20\,°C$) was achieved after approx. 200 s, which is quite an impressive value. This fast heat build-up is possible thanks to the fully closed fresh air flap, which has the drawback of slightly degraded air quality (above 1000 ppm; limited for a short time). The air quality is improved immediately after the cabin temperature settles and then it is kept approximately at the reference value of 900 ppm.

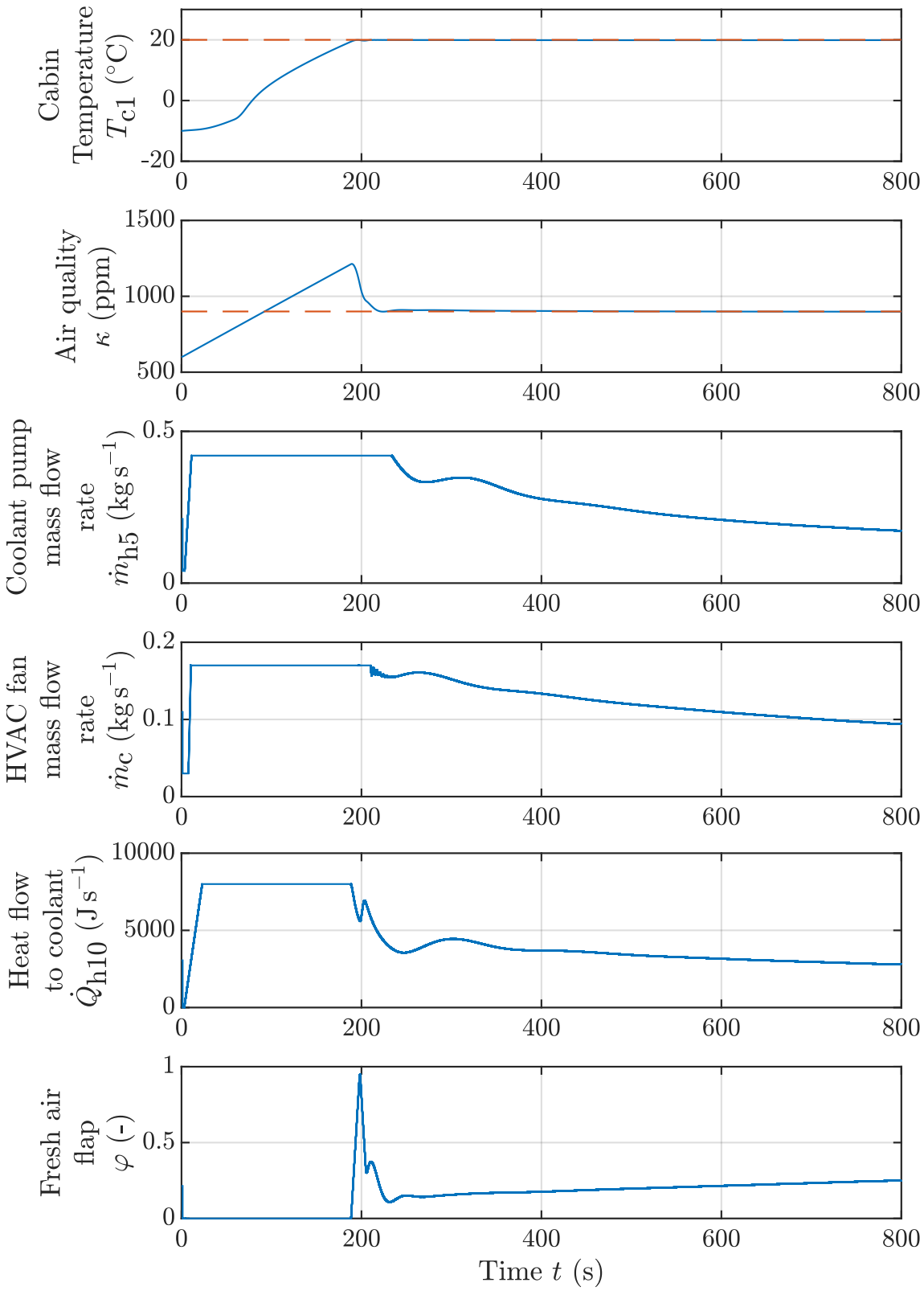

Fig. 3.5: NMPC PIL simulation of cabin heat build-up with ambient temperature $T_{c5} = -10\,°C$, two passengers inside the cabin and no solar heat flow

4 Electro-thermal flows optimization

The overall vehicle thermal system (Fig. 2.1) was divided into three subsystems: Heating, Ventilation and Air Conditioning (HVAC) (also includes Refrigeration (HVAC&R)), High-Voltage Battery (HvBat) and E-Drive (ED).

For each subsystem, a set of Thermal Functions were defined. Thermal Function (TF) is a term used for a set of actuators' values and control rules. Each TF is intended for different situations defined by ambient conditions, heating/cooling request and current values of VTMS states (TES status, coolant temperature, etc.).

Thermal Decision Controller (TDC) is a name for a set of algorithms that are responsible for the selection of appropriate Thermal Function (TF). Two versions of TDC were developed, a Basic Thermal Decision Controller (BTDC) and a Model Predictive Thermal Decision Controller (MPTDC).

4.1 Model Predictive Thermal Decision Controller

This section describes an advanced algorithm for Thermal Function selection. The algorithm uses a Model Predictive Control (MPC) approach applied to the hybrid system - a dynamic system combined with discrete-valued variables or a state machine.

The theory of hybrid MPC is quite well established and in this thesis, it was used for the development of the decision-making algorithm. The system (or its simplified representation) and its modes are described by the PWA model and MPC is then used for the selection of optimal mode during system operation.

4.1.1 DMPC for PWA systems

We propose to use MPC for selection of optimal control strategy of complex t-invariant non-linear system

$$\mathbf{x}_{k+1} = \mathbf{f}(\mathbf{x}_k, \mathbf{u}_k), \tag{4.1}$$

$$\mathbf{y}_k = \mathbf{h}(\mathbf{x}_k, \mathbf{u}_k), \tag{4.2}$$

with $\mathbf{x}$, $\mathbf{u}$ and $\mathbf{y}$ being the vector of states, inputs and outputs, $\mathbf{f}(\cdot)$ state update function and $\mathbf{h}(\cdot)$ the output function. Commonly, such a system has some binary $\mathbf{u}_k^{\mathrm{b}} \in \{0,1\}^{n_{\mathrm{b}}}$ and/or integral $\mathbf{u}_k^{\mathrm{i}} \in \mathbb{Z}^{n_{\mathrm{i}}}$ actuators (valves, switches, constant/step speed drives, etc.), which together form modes of the system. Under these modes, the system is operated and possibly continuously controlled by continuous inputs $\mathbf{u}_k^{\mathrm{r}} \in \mathbb{R}^{n_{\mathrm{r}}}$. Usually, the switching between modes is somehow constrained (switching frequency, etc.). Then the input vector can be written as

$$\mathbf{u}_k = \begin{bmatrix} \mathbf{u}_k^{\mathrm{b}} \\ \mathbf{u}_k^{\mathrm{i}} \\ \mathbf{u}_k^{\mathrm{r}} \end{bmatrix}. \tag{4.3}$$

We assume that we can find a simplified model of such a system in the form of a general high-level PWA dynamic model (incorporating e.g. generalized thermal flows, material flows, electric power flows, etc.). We define domain $\mathbb{U}_i^{\mathrm{b}}$ of i^{th} binary input variable u_i^{b} as

$$u_i^{\mathrm{b}} \in \mathbb{U}_i^{\mathrm{b}} \triangleq \{0,1\} \tag{4.4}$$

and similarly, the domain $\mathbb{U}_i^{\mathrm{i}}$ of i^{th} integral input variable u_i^{i} as

$$u_i^{\mathrm{i}} \in \mathbb{U}_i^{\mathrm{i}} \subset \mathbb{Z}, \tag{4.5}$$

with the assumption of reasonably constrained domains of integral variables. We then list all the binary and integral inputs combinations

$$\mathbf{M} = \prod_{i=1}^{n_{\mathrm{b}}} \mathbb{U}_i^{\mathrm{b}} \times \prod_{i=1}^{n_{\mathrm{i}}} \mathbb{U}_i^{\mathrm{i}} \tag{4.6}$$

and select their allowed combinations $\mathbf{M}_{\mathrm{a}} \subseteq \mathbf{M}$. Each item $m \in \mathbf{M}_{\mathrm{a}}$ is referred to as an *operating mode* and it is necessary to find an affine (or linear) dynamic description of the system within each operating mode. All the operating modes must have common vectors of inputs $\mathbf{u}^*$, states $\mathbf{x}^*$ and outputs $\mathbf{y}^*$, which, in general, will not be the same as the original vectors $\mathbf{u}$, $\mathbf{x}$ and $\mathbf{y}$ (they might be similar for simple systems). We suppose that all the operating modes share the same input and state constraints

$$\mathbf{E}\mathbf{x}_k^* + \mathbf{F}\mathbf{u}_k^* \leq \mathbf{G}, \tag{4.7}$$

which define the polyhedron

$$\mathcal{P} \subset \mathbb{R}^{n_{x^*}+n_{u^*}}. \tag{4.8}$$

Imagine that we succeed to find the dynamic description of i^{th} operating mode ($i = 1, 2 \ldots |\mathbf{M}_{\text{a}}|$) in affine form as

$$\mathbf{x}^*_{k+1} = \mathbf{A}_i \mathbf{x}^*_k + \mathbf{B}_i \mathbf{u}^*_k + \mathbf{f}^{\text{c}}_i, \tag{4.9}$$

$$\mathbf{y}^*_k = \mathbf{C}_i \mathbf{x}^*_k + \mathbf{D}_i \mathbf{u}^*_k + \mathbf{g}^{\text{c}}_i, \tag{4.10}$$

$$\text{for } \begin{bmatrix} \mathbf{x}^*_k \\ \mathbf{u}^*_k \end{bmatrix} \in \mathcal{P}_i, \tag{4.11}$$

then several possibilities can happen:

- $\mathcal{P}_i = \mathcal{P}$ or $\mathcal{P}_i \supset \mathcal{P}$, which means that the current operating mode is also a *PWA system mode*
- $\mathcal{P}_i \subset \mathcal{P}$, which means that there exist at least two operating submodes within the current operating mode

In the second case, we denote the polyhedron $\mathcal{P}_i$ as $\mathcal{P}_{i1}$ and we need to find an affine dynamic model for $\mathcal{P}_{i2} \triangleq \mathcal{P} \backslash \mathcal{P}_{i1}$. We repeat this step and stop the searching if the condition

$$\bigcup_{j=1}^{s_i} \mathcal{P}_{ij} \supseteq \mathcal{P} \tag{4.12}$$

is fulfilled, which means that the whole constrained state-input space is covered by s_i submodes models. Each submode then becomes a new *PWA system mode*. This procedure is repeated for each operating mode (i.e. i is incremented and we try to find a model within this operating mode using the steps above).

The distinction between operating modes is proposed based on dummy input $\tilde{u}$, which denotes the item $m \in \mathbf{M}_{\text{a}}$. The input $\tilde{u}$ can be defined as needed, we propose $\tilde{u} \in \mathbb{N}$ and a single value of $\tilde{u}$ is assigned to each operating mode, for the i^{th} operating mode $\tilde{u} = i$.

The PWA system input vector $\mathbf{u}^*$ is extended by adding the dummy input $\tilde{u}$

$$\bar{\mathbf{u}} = \begin{bmatrix} \tilde{u} \\ \mathbf{u}^* \end{bmatrix} \tag{4.13}$$

and the polyhedron $\mathcal{P}$ has to be extended to

$$\mathcal{P}^* = \mathcal{P} \times \{1, 2 \ldots |\mathbf{M}_{\text{a}}|\}, \tag{4.14}$$

that is a polyhedral union of PWA system modes polyhedrons

$$\mathcal{P}^* = \bigcup_{i=1}^{|\mathbf{M}_\mathrm{a}|} \mathcal{P}_i^*, \tag{4.15}$$

where

$$\mathcal{P}_i^* = \begin{cases} \mathcal{P} \times i & \text{if } s_i = 1 \\ (\mathcal{P} \times i) \cap \bigcup_{j=1}^{s_i} \mathcal{P}_{ij}^* & \text{if } s_i > 1 \end{cases}, \tag{4.16}$$

where $i \in \{1, 2 \dots |\mathbf{M}_\mathrm{a}|\}$ and $\mathcal{P}_{ij}^* = \mathcal{P}_{ij} \times i$. For simplification of further text, we will denote $\mathcal{P}_i^*$ with no operating submodes as $\mathcal{P}_{i1}^*$. By adjusting matrices $\mathbf{B}$ and $\mathbf{D}$ according to (4.13)

$$\mathbf{B}^* = \begin{bmatrix} \mathbf{0} & \mathbf{B} \end{bmatrix}, \qquad \mathbf{D}^* = \begin{bmatrix} \mathbf{0} & \mathbf{D} \end{bmatrix} \tag{4.17}$$

we get the description of the simplified system in PWA form

$$\mathbf{x}_{k+1}^* = \begin{cases} \mathbf{A}_{11}\mathbf{x}_k^* + \mathbf{B}_{11}^*\bar{\mathbf{u}}_k + \mathbf{f}_{11}^\mathrm{c} & \text{if } (\mathbf{x}_k^*, \bar{\mathbf{u}}_k) \in \mathcal{P}_{11} \\ \vdots & \vdots \\ \mathbf{A}_{|\mathbf{M}_\mathrm{a}|s_\mathrm{max}}\mathbf{x}_k^* + \mathbf{B}_{|\mathbf{M}_\mathrm{a}|s_\mathrm{max}}^*\bar{\mathbf{u}}_k + \mathbf{f}_{|\mathbf{M}_\mathrm{a}|s_\mathrm{max}}^\mathrm{c} & \text{if } (\mathbf{x}_k^*, \bar{\mathbf{u}}_k) \in \mathcal{P}_{|\mathbf{M}_\mathrm{a}|s_\mathrm{max}} \end{cases}, \tag{4.18}$$

$$\mathbf{y}_k^* = \begin{cases} \mathbf{C}_{11}\mathbf{x}_k^* + \mathbf{D}_{11}^*\bar{\mathbf{u}}_k + \mathbf{g}_{11}^\mathrm{c} & \text{if } (\mathbf{x}_k, \bar{\mathbf{u}}_k) \in \mathcal{P}_{11} \\ \vdots & \vdots \\ \mathbf{C}_{|\mathbf{M}_\mathrm{a}|s_\mathrm{max}}\mathbf{x}_k^* + \mathbf{D}_{|\mathbf{M}_\mathrm{a}|s_\mathrm{max}}^*\bar{\mathbf{u}}_k + \mathbf{g}_{|\mathbf{M}_\mathrm{a}|s_\mathrm{max}}^\mathrm{c} & \text{if } (\mathbf{x}_k^*, \bar{\mathbf{u}}_k) \in \mathcal{P}_{|\mathbf{M}_\mathrm{a}|s_\mathrm{max}} \end{cases}, \tag{4.19}$$

where

$$s_\mathrm{max} \triangleq \max_{i=1}^{|\mathbf{M}_\mathrm{a}|} s_i \tag{4.20}$$

denotes a maximal number of submodes over all the operating modes and $|\mathbf{M}_\mathrm{a}|$ is the cardinality of the set of allowed operating modes.

Usually, the PWA systems are used to describe the behavior of a real system concerning different dynamics for different operating points. Here we extend the usage for decision system, which can optimize system energy consumption with compliance to references and system constraints.

The modes of PWA system here represent different control strategies or different system configurations (for example heat pump source/sink configuration; cooling/heating distinction for different systems; for HEV type of propulsion - petrol/electric etc.).

Then we propose to use MPC for selection of system mode and thus values of binary and integral actuators and at the same time the control strategy of the continuously controlled actuators (set of controllers etc.).

MPC is employed to find, which mode of system in (4.18) - (4.19) is optimal in terms of reference tracking, complying with the system constraints and power consumption minimization, all defined by cost function and model constraints. The cost function is used in the form

$$J_N(\mathbf{x}_0, \hat{\mathbf{u}}) = \sum_{k=0}^{N-1} \left[(\mathbf{x}_k - \mathbf{r}_k)^\intercal \mathbf{Q} (\mathbf{x}_k - \mathbf{r}_k) + \bar{\mathbf{u}}_k^\intercal \mathbf{R} \bar{\mathbf{u}}_k + \Delta \bar{\mathbf{u}}_k^\intercal \mathbf{S} \Delta \bar{\mathbf{u}}_k \right], \tag{4.21}$$

with $\mathbf{x}$ being the state vector, $\mathbf{r}$ the state references vector and $\bar{\mathbf{u}}$ the modified PWA system input vector. The matrices $\mathbf{Q}$, $\mathbf{R}$ and $\mathbf{S}$ are the penalization matrices for state error, inputs, and input change rate. The matrices $\mathbf{R}$ and $\mathbf{S}$ contain element related to input $\tilde{u}$ on position [1,1]

$$\mathbf{R} = \begin{bmatrix} R_{11} & \dots \\ \vdots & \ddots \end{bmatrix}, \qquad \mathbf{S} = \begin{bmatrix} S_{11} & \dots \\ \vdots & \ddots \end{bmatrix} \tag{4.22}$$

and these elements can be used for influencing the mode switching. Firstly, if we sort the operating modes from best to worst (from any perspective), using R_{11} the mode selection can be adjusted. Secondly, the mode switching rate can be penalized using S_{11}, which needs to be tuned to ensure the desired switching behavior.

Remark. *The cost function (4.21) is not used for optimizations in this form, as the PWA system (and also the penalization matrices) needs to be converted into MLD or LCP system to be usable with available solvers. However, the form of (4.21) is useful for its clearness and thus it is used for explanation of dummy input penalization.*

The result of the optimization of (4.21) (or its equivalent for MLD or LCP system) is a vector of predicted optimal inputs $\hat{\mathbf{u}}$. If we consider standard receding horizon control (RHC) on prediction horizon N, only the first step control values $\hat{\mathbf{u}}_k$ are applied on a controlled system and the rest of predicted values $(\hat{\mathbf{u}}_{k+1} \dots \hat{\mathbf{u}}_{k+N-1})$ are discarded. We can reuse this approach and extend it by discarding all the predicted inputs except $\tilde{u}_k$, which is used for operating mode selection.

The control of actuators is then managed by low-level algorithms, which ensure precise reference tracking, disturbance rejection, and other tasks. As this approach is aimed at a complex non-linear system (tens of inputs, up to tens of thousands of states), the MPC cannot be solved for every real input of the system because of high computational demands.

We refer to this approach of high-level system modes switching as the Decision Model Predictive Control (DMPC).

4.1.2 DMPC for FEV VTMS

Overview of a whole VTMS system is in Fig. 2.1 and for this system, there are many possible combinations of binary actuators. So, in this case, the procedure was slightly different from the theoretical procedure described above.

The system was divided into three subsystems - HVAC, HvBat and ED. For each subsystem, several Thermal Functions (TF) were defined to allow the required functionality. Then compatibility of TFs between subsystems was analyzed and a table of compatible TFs was created. Still there remained a lot of possible combinations (approx. 20 – 30), thus we assembled preferred combinations of TF for the subsystems and each combination is called Overall Thermal Function (OTF) and described by a number (124, 211, 224, 373, 463, 511, 524). The first position denotes HVAC TF, the second stands for HvBat TF and the third belongs to ED TF. The list of OTF is presented in Tab. 4.1.

Example. *OTF 373 means a combination of HVAC TF3, HvBat TF7, and ED TF3.*

VTMS PWA model

The PWA model of VTMS energy flows was assembled in a general form as shown in Fig. 4.1 and it can be described by following set of equations

Tab. 4.1: Overall Thermal Functions overview

	HVAC	HV Battery	E-Drive
OTF 124	cooling by ambient air	cooling by ambient air	cooling by ambient air
OTF 211	cooling by VCRS with ambient air and TES as heat sinks	cooling by VCRS with ambient air and TES as heat sinks	cooling by ambient air
OTF 224	cooling by VCRS with ambient air and TES as heat sinks	cooling by ambient air	cooling by ambient air
OTF 373	heating by VCRS with coolant as a heat source	cooling by coolant and VCRS	cooling by coolant and VCRS
OTF 463	heating by VCRS with ambient air as a heat source	cooling by coolant	cooling by coolant
OTF 511	cooling by VCRS with ambient air as a heat sink	cooling by VCRS with ambient air as a heat sink	cooling by ambient air
OTF 524	cooling by VCRS with ambient air as a heat sink	cooling by ambient air	cooling by ambient air

$$C_{\text{cab}}\frac{\mathrm{d}T_{\text{cab}}}{\mathrm{d}t} = \dot{Q}_{\text{amb0}} - \dot{Q}_{\text{loss}} - \dot{Q}_{\text{amb1}} + \dot{Q}_{\text{cmpr0}} - \dot{Q}_{\text{TES1}} + \dot{Q}_{\text{co0}}, \tag{4.23}$$

$$C_{\text{co}}\frac{\mathrm{d}T_{\text{co}}}{\mathrm{d}t} = -\dot{Q}_{\text{co0}} + \dot{Q}_{\text{TES0}} - \dot{Q}_{\text{co1}} + \dot{Q}_{\text{PTC}} - \dot{Q}_{\text{amb3}} + \dot{Q}_{\text{ED1}} + \dot{Q}_{\text{bat1}}, \tag{4.24}$$

$$C_{\text{bat}}\frac{\mathrm{d}T_{\text{bat}}}{\mathrm{d}t} = \dot{Q}_{\text{bat0}} - \dot{Q}_{\text{bat1}}, \tag{4.25}$$

$$C_{\text{ED}}\frac{\mathrm{d}T_{\text{ED}}}{\mathrm{d}t} = \dot{Q}_{\text{ED0}} - \dot{Q}_{\text{ED1}} - \dot{Q}_{\text{amb2}}, \tag{4.26}$$

$$\frac{\mathrm{d}U_{\text{TES}}}{\mathrm{d}t} = \dot{Q}_{\text{TES1}} - \dot{Q}_{\text{TES0}} + \dot{Q}_{\text{co1}} + \dot{Q}_{\text{cmpr2}}, \tag{4.27}$$

$$\frac{\mathrm{d}T_{\text{amb}}}{\mathrm{d}t} = 0, \tag{4.28}$$

$$y_{\text{cab}} = T_{\text{cab}}, \tag{4.29}$$

$$y_{\text{bat}} = T_{\text{bat}}, \tag{4.30}$$

which can be simplified for each OTF, discretized and written in state-space

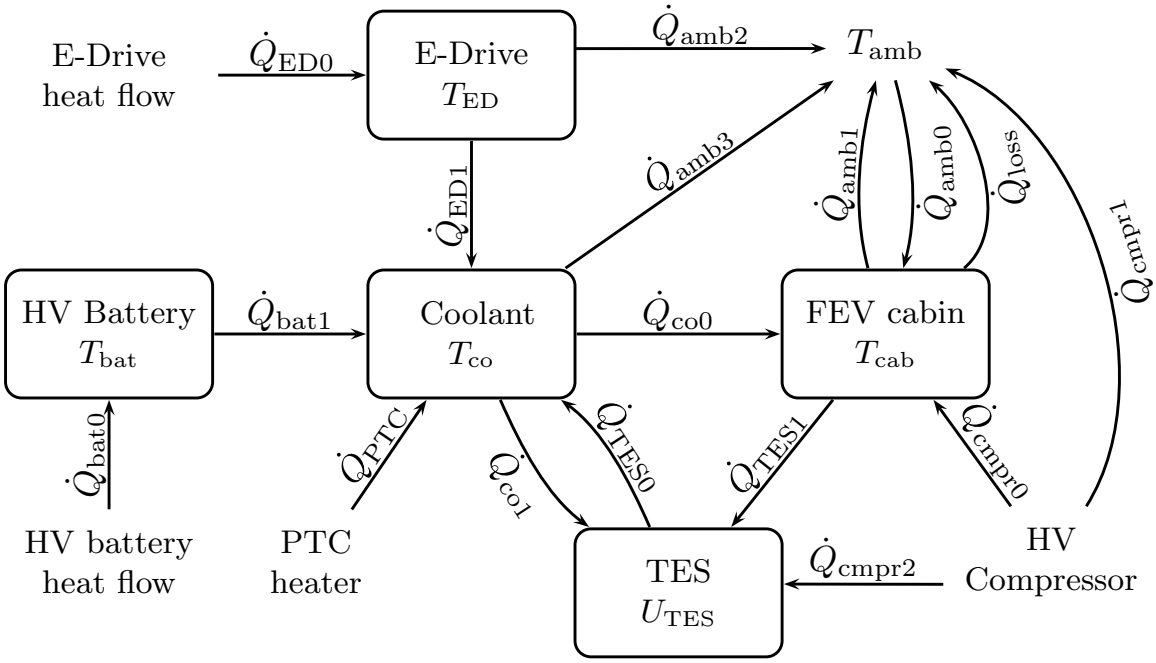

Fig. 4.1: Diagram of FEV simplified heat flows

form

$$\mathbf{x}^*_{k+1} = \mathbf{A}\mathbf{x}^*_k + \mathbf{B}^*\bar{\mathbf{u}}_k + \mathbf{f}^{\mathrm{c}}, \tag{4.31}$$

$$\mathbf{y}^*_k = \mathbf{C}\mathbf{x}^*_k + \mathbf{D}^*\bar{\mathbf{u}}_k + \mathbf{g}^{\mathrm{c}}, \tag{4.32}$$

where

$$\mathbf{x}^* = \begin{bmatrix} T_{\mathrm{cab}} & T_{\mathrm{co}} & T_{\mathrm{bat}} & T_{\mathrm{ED}} & U_{\mathrm{TES}} & T_{\mathrm{amb}} \end{bmatrix}^\intercal, \tag{4.33}$$

$$\bar{\mathbf{u}} = \begin{bmatrix} OTF & u_{\mathrm{cmpr}} & u_{\mathrm{hf}} & u_{\mathrm{cc}} & u_{\mathrm{cb}} & u_{\mathrm{ptc}} \end{bmatrix}^\intercal, \tag{4.34}$$

$$\mathbf{y}^* = \begin{bmatrix} y_{\mathrm{cab}} & y_{\mathrm{bat}} \end{bmatrix}^\intercal. \tag{4.35}$$

For each operating mode (represented by OTF) a dynamic affine model with the common state, input, and output vector is being formulated by omitting and expressing the thermal flows taken from the general PWA model. The single OTF models are shown in the appendix of the doctoral thesis. The models are assembled in a continuous-time domain and then discretized (not shown within this text).

Here we remind that the PWA model does not aspire to be the exact representation of VTMS, it only serves as a high-level approximation for decision purposes. Also, the control vector obtained from the MPC controller should

be discarded except the OTF indicator and the actuators need to be controlled by another set of low-level algorithms in the final implementation.

MPTDC implementation

MPTDC algorithms were tested only in simulations, as the demonstration vehicle was not finished. MPT toolbox [21] in combination with MATLAB and Simulink was used for hybrid MPC controller design, simulations and code generation. Also, Hybrid Toolbox [22] provides similar features and could be used for this purpose.

MPC algorithms were verified in Processor in the Loop (PIL) simulation. The generated code of controller was implemented into the Infineon AURIX Tricore TC299TF microcontroller unit (MCU), placed on AURIX Starter Kit TC299. The MCU contains three cores running at 300 MHz, 8 MB FLASH (4x2 MB) and 728 kB RAM. Due to FLASH memory limitation, it was possible to implement an MPC controller with a prediction horizon up to $N = 3$.

In Fig. 4.2 there is a result of MPTDC PIL simulation under winter condition with charged PCM. The MPC algorithm selects the appropriate OTF based on constraints and references compliance. For approximately 2200 s the OTF 373 is selected and waste heat and PCM are fully utilized. After exhaustion of TES, the system switches between OTF 373e and 463, waste heat recovery function and heating with ambient air as a heat source respectively.

It is noticeable that the PTC heater is occasionally requested to support the cabin heating by adding some heat to the coolant (power of up to 200 W). This helps to keep the system in the waste heat recovery mode (OTF 373 or 373e) and thus the overall power consumption is lower, than if the system falls into heat pump mode with ambient air as a heat source.

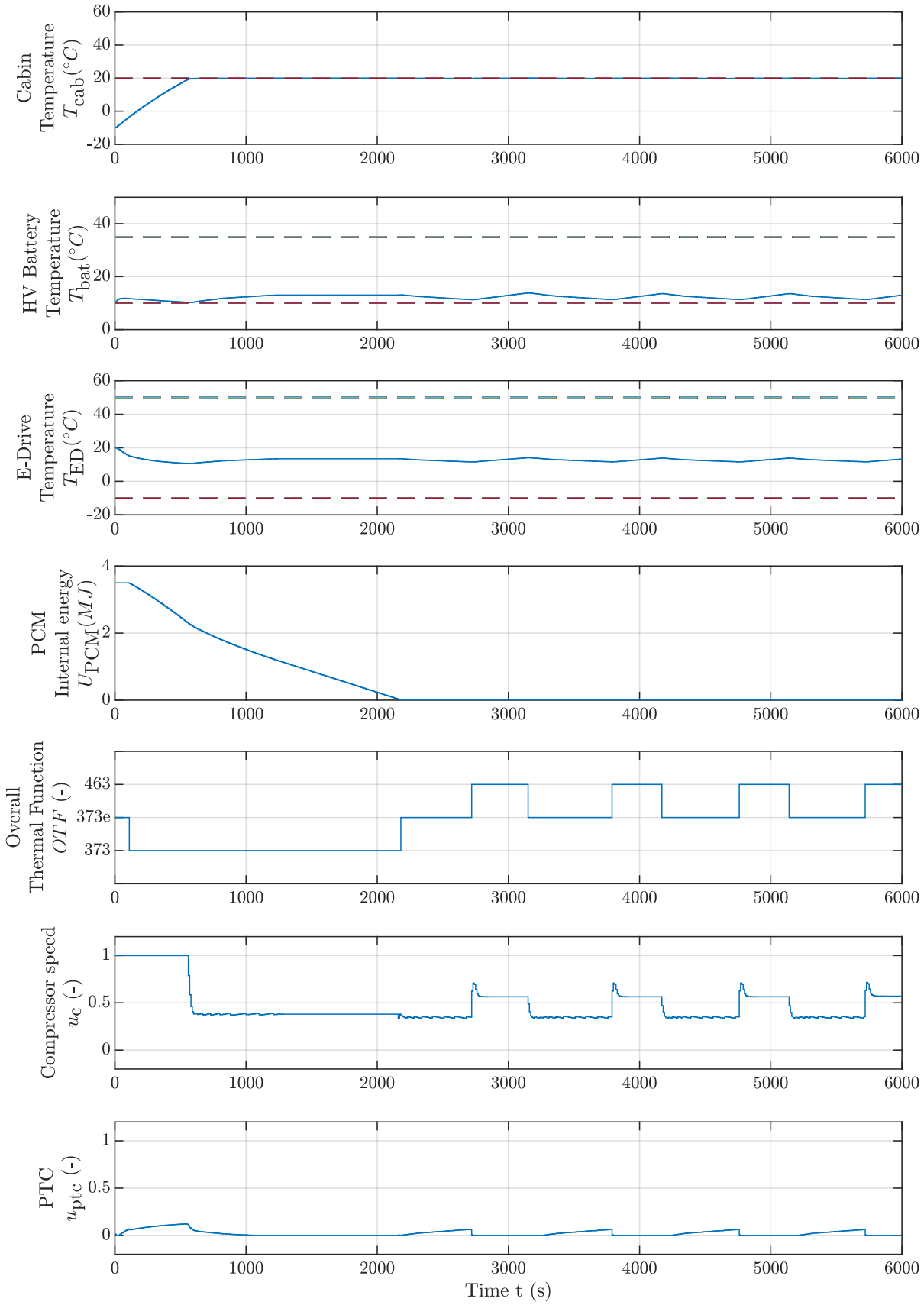

Fig. 4.2: MPTDC PIL simulation under winter condition with $T_{amb} = -10\,°C$, $\dot{Q}_{ED0} = 600\,W$ and $\dot{Q}_{bat0} = 400\,W$

5 Conclusion

This thesis deals with modeling and control of the innovative Vehicle Thermal Management System (VTMS) for Fully Electric Vehicle (FEV). The topic is very interesting from the FEV range perspective, as it can help to avoid mileage decrease under adverse ambient conditions without losing the user comfort during driving. Moreover, if we consider other EV types (PHEV, FCEV) or even different modes of transportation, the optimization of energy consumption is important not only from the range point of view but also from the general energy-saving perspective.

The models and control algorithms were developed for an innovative VTMS layout, which enables many operating modes, including heat pump functionality with a different heat source and sink configurations. However, the methods and approaches can be applied to different VTMS layouts and are not even limited to automotive applications and could be used in other areas.

As the proposed VTMS layout allows many operating modes ("Thermal Functions"), it was needed to develop an algorithm for real-time mode selection.

The proposed solution uses a Hybrid MPC approach modification, which was formally described as Decision Model Predictive Control. This method is based on a set of highly simplified FEV thermal flows dynamic models, with each representing one Overall Thermal Function. The models were united into a single piecewise affine model and Hybrid MPC is used to select the appropriate Overall Thermal Function.

Then within each Thermal Function, a set of control algorithms was designed to fulfill the requirements on defined references. That means VCRS control, cabin temperature control, HV Battery temperature control and E-Drive temperature control.

For selected control problems more advanced control algorithms were prepared. First of them is cabin temperature control in combination with cabin air quality control realized by Non-linear Model Predictive Control. This integrated approach brings convenient cabin air quality and temperature together with the minimization of electric power consumption. This control approach was tested using PIL simulation, as the real-world testing would require a vehicle cabin, which was not available on the test bench.

The model-based electronic expansion valve control algorithm was designed

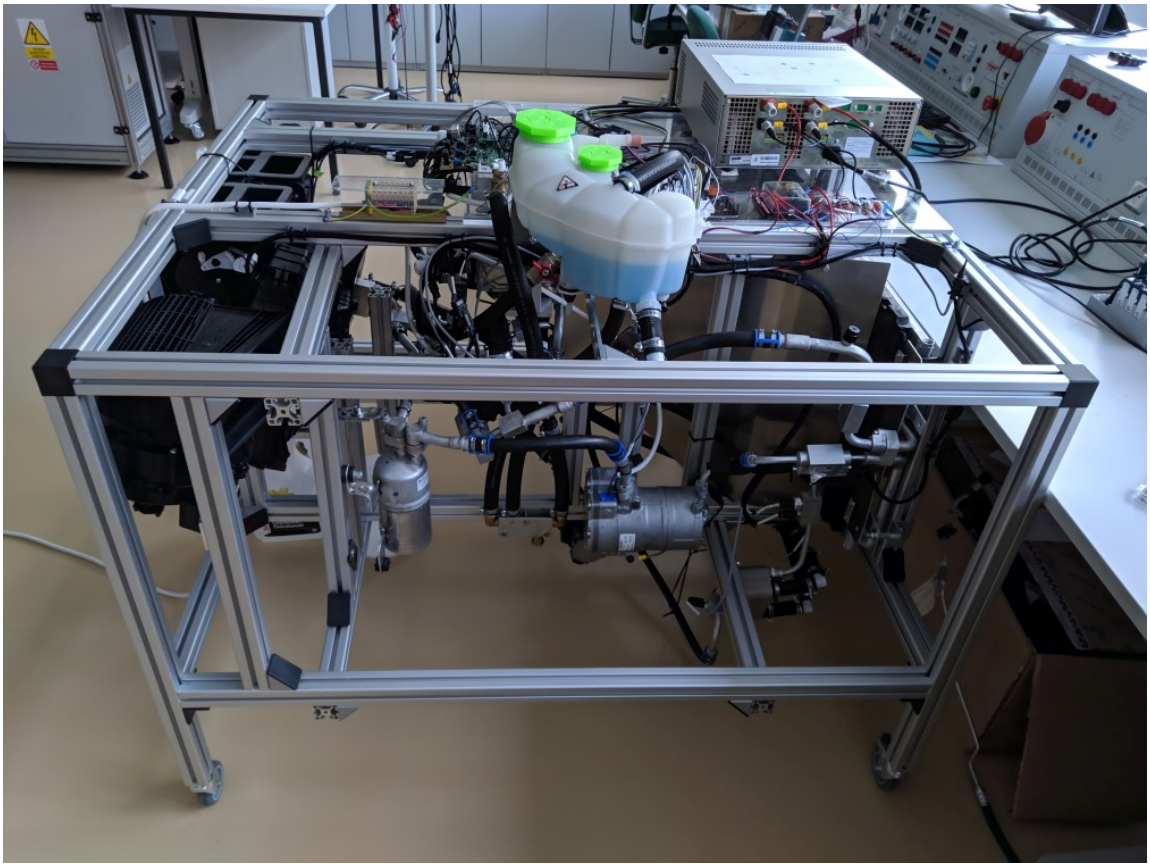

Fig. 5.1: Test bench photo

for Vapor Compression Refrigeration System (VCRS) subcooling control. This approach uses a compressor refrigerant mass flow rate estimator in combination with an expansion valve mass flow rate equation and predicts the valve steady-state opening degree. To reject the disturbances and inaccuracies of this approach the model-based EXV controller was complemented by the PI controller. The algorithm was tested on the test bench (Fig. 5.1) and it brings substantial improvement of VCRS performance especially during system start-up. This control method could be improved by including the condenser model, which could refine the refrigerant mass flow rate estimation.

Future research and development could focus on vehicle cabin air dehumidification as the proposed VTMS layout could allow energy-efficient operation within this mode. Also, we can see possible improvements in decisive hybrid MPC, for example, implicit implementation could bring longer prediction horizon (if considering large sampling times, which provide enough time for online optimizations).

Bibliography

[1] W. Adaileh and A. Alahmer, "Recovery of Exhaust Waste Heat for ICE Using the Beta Type Stirling Engine," *Journal of Energy*, vol. 2015, p. Article ID 495418, 2015.

[2] K. T. Chau and C. C. Chan, "Emerging Energy-Efficient Technologies for Hybrid Electric Vehicles," *Proceedings of the IEEE*, vol. 95, pp. 821–835, Apr. 2007.

[3] M. Åhman, "Primary energy efficiency of alternative powertrains in vehicles," *Energy*, vol. 26, pp. 973–989, Nov. 2001.

[4] J. R. M. Delos Reyes, R. V. Parsons, and R. Hoemsen, "Winter Happens: The Effect of Ambient Temperature on the Travel Range of Electric Vehicles," *IEEE Transactions on Vehicular Technology*, vol. 65, pp. 4016–4022, June 2016.

[5] G. Mimberg and C. Massonet, "Battery concept to minimize the climate-related reduction of electric vehicles driving range," in *2017 12th International Conference on Ecological Vehicles and Renewable Energies, EVER 2017*, Institute of Electrical and Electronics Engineers Inc., May 2017.

[6] N. Meyer, I. Whittal, M. Christenson, and A. Loiselle-Lapointe, "The Impact of Driving Cycle and Climate on Electrical Consumption & Range of Fully Electric Passenger," in *EVS26 International Battery, Hybrid and Fuel Cell Electric Vehicle Symposium*, 2012.

[7] Z. Zhang, J. Wang, X. Feng, L. Chang, Y. Chen, and X. Wang, "The solutions to electric vehicle air conditioning systems: A review," *Renewable and Sustainable Energy Reviews*, vol. 91, pp. 443–463, Aug. 2018.

[8] Z. Zhao and N. Yu, "The application of advanced control technologies in air conditioning system–a review," *Advances in Building Energy Research*, vol. 11, no. 1, pp. 52–66, 2017.

[9] O. Ekren, S. Sahin, and Y. Isler, "Comparison of different controllers for variable speed compressor and electronic expansion valve," *International Journal of Refrigeration*, vol. 33, pp. 1161–1168, Sept. 2010.

[10] X. Yin and S. Li, "Energy efficient predictive control for vapor compression refrigeration cycle systems," *IEEE/CAA Journal of Automatica Sinica*, vol. 5, pp. 953–960, Sept. 2018.

[11] M. Wallace, P. Mhaskar, J. House, and T. Salsbury, "Offset-free model predictive controller of a heat pump," in *2014 American Control Conference*, pp. 2247–2252, IEEE, June 2014.

[12] M. Gräber, C. Kirches, J. P. Schlöder, and W. Tegethoff, "Nonlinear Model Predictive Control of a Vapor Compression Cycle based on First Principle Models," *IFAC Proceedings Volumes*, vol. 45, no. 2, pp. 258–263, 2012.

[13] X. H. Yin and S. Y. Li, "Model Predictive Control for Vapor Compression Cycle of Refrigeration Process," *International Journal of Automation and Computing*, vol. 15, pp. 707–715, Dec. 2018.

[14] A. Goyal, M. A. Staedter, and S. Garimella, "A review of control methodologies for vapor compression and absorption heat pumps," *International Journal of Refrigeration*, vol. 97, pp. 1–20, Jan. 2019.

[15] G. Pottker, P. Hrnjak, and P. H. Pottker Gustavo, "Effect of Condenser Subcooling of the Performance of Vapor Compression Systems: Experimental and Numerical Investigation," in *International Refrigeration and Air Conditioning Conference*, vol. 50, pp. 1–10, 2012.

[16] L. Xu and P. Hrnjak, "Potential for Improving Efficiency by Controlling Subcooling in Residential A / C System," *International Refrigeration and Air Conditioning Conference*, pp. 1–10, 2014.

[17] M. Pitarch, E. Hervas-Blasco, E. Navarro-Peris, J. Gonzálvez-Maciá, and J. M. Corberán, "Evaluation of optimal subcooling in subcritical heat pump systems," *International Journal of Refrigeration*, vol. 78, pp. 18–31, June 2017.

[18] E. Hervas-Blasco, M. Pitarch, E. Navarro-Peris, and J. M. Corberán, "Study of different subcooling control strategies in order to enhance the

performance of a heat pump," *International Journal of Refrigeration*, vol. 88, pp. 324–336, Apr. 2018.

[19] C. Goh, L. Kamarudin, S. Shukri, N. Abdullah, and A. Zakaria, "Monitoring of carbon dioxide (CO2) accumulation in vehicle cabin," in *2016 3rd International Conference on Electronic Design (ICED)*, pp. 427–432, IEEE, Aug. 2016.

[20] L. Grüne and J. Pannek, *Nonlinear Model Predictive Control: Theory and Algorithms*. 2011.

[21] M. Herceg, M. Kvasnica, C. N. Jones, and M. Morari, "Multi-Parametric Toolbox 3.0," in *2013 European Control Conference (ECC)*, pp. 502–510, IEEE, July 2013.

[22] A. Bemporad, "Hybrid Toolbox - User's Guide." Available at: http://cse.lab.imtlucca.it/~bemporad/hybrid/toolbox, 2004.

Curriculum vitæ

Education

Cybernetics, Control and Measurements 2015-now
Doctoral degree
Brno University of Technology
Faculty of Electrical Engineering and Communication

Cybernetics, Control and Measurements 2013-2015
Master's degree
Brno University of Technology
Faculty of Electrical Engineering and Communication

Automation and Measurement 2009-2013
Bachelor's degree
Brno University of Technology
Faculty of Electrical Engineering and Communication

Teaching and advising

Faculty of Electrical Engineering and Communication
Modeling and Simulation
Control Theory 2
M. Chromiak, "Tepelný model kabiny automobilu pro HIL simulaci" bachelor's thesis, Vysoké učení technické v Brně, Brno, 2018.

Faculty of Business and Management
Theory of Systems

Projects

H2020 AutoDrive - Advancing fail-aware, fail-safe, and fail-operational electronic components, systems, and architectures for fully automated driving to make future mobility safer, affordable, and end-user acceptable.

H2020 OSEM-EV - Optimised and Systematic Energy Management in Electric Vehicles

H2020 3Ccar - Integrated Components for Complexity Control in affordable electrified cars

MATERIS - Podpora rozvoje kvalitních týmů výzkumu a vývoje v oblasti materiálových věd

FEKT-S-14-2429 - The research of new control methods, measurement procedures and intelligent instruments in automation

FEKT-S-17-4234 - Industry 4.0 in automation and cybernetics

Published papers

[23] J. Glos, P. Václavek, and P. Blaha, "Energy efficient control of a heat pump in fully electric vehicle," in *Proceedings of the 7th European Transport Research Arena 2018*, (Wien), 2018.

[24] J. Glos, "FMUtoolbox cross check implementation and FMI Standard compliance results," in *Proceedings of the 24th Conference STUDENT EEICT 2018*, (Brno), pp. 403–407, Vysoké učení technické v Brně, Fakulta elektrotechniky a komunikačních technologií, 2018.

[25] M. Hütter, M. Nica, E. Sumann, J. Tao, J. Glos, M. Gepp, M. Helwig, H.-F. D. C. Garcia, A. Bacar, and N. De-Guyenro, "Impact of thermal-electric networks on the usability of EVs based on a study with a C-

segment car," in *Proceedings of the 7th European Transport Research Arena 2018*, 2018.

[26] J. Glos and F. Šolc, "Determination of optimum high-side pressure of R744 automotive heat pump using Fibonacci search method," in *Proceedings of the 2017 IEEE International Symposium on Industrial Electronics*, pp. 448–453, IEEE, 2017.

[27] J. Glos and P. Václavek, "Efficient control of automotive R744 heat pump using Nelder-Mead simplex method," in *Proceedings of the 2017 IEEE International Conference on Industrial Technology*, pp. 785–790, IEEE, 2017.

[28] J. Glos and P. Václavek, "Nelder-Mead algorithm based control strategy for CO2 heat pump," in *Book of Abstracts CEITEC PhD Retreat II.*, (Brno), pp. 70–70, Masaryk University, 2017.

[29] J. Glos, "FMU Toolbox for Matlab/Simulink," in *Proceedings of the 22st Conference STUDENT EEICT 2016*, pp. 426–430, Vysoké učení technické v Brně, Fakulta elektrotechniky a komunikačních technologií, 2016.

[30] J. Glos, "Využití modelů v jazyce Modelica v prostředí Matlab-Simulink," in *Proceedings of the 21st Conference STUDENT EEICT 2015*, (Brno), pp. 310–312, Vysoké učení technické v Brně, Fakulta elektrotechniky a komunikačních technologií, 2015.

[31] J. Glos, "RefToolbox - refrigeration toolbox for MATLAB/Simulink," in *Proceedings of the 25th Conference STUDENT EEICT 2019*, (Brno), pp. 551–555, Vysoké učení technické v Brně, Fakulta elektrotechniky a komunikačních technologií, 2019.

ABSTRACT

In fully electric vehicles a systematic control of thermal and electric flows is becoming very important as there is not enough waste heat for cabin heating. To avoid vehicle driving range decrease under winter condition it is necessary to employ devices allowing minimization of energy needed for cabin heating (e.g. heat pump, thermal energy storage). It is required to implement control algorithms for such devices to ensure their optimal operation. In summer conditions it is also necessary to control thermal flows to avoid excessive battery discharge due to vehicle thermal management. This work deals with control algorithms design as well as with the development of decision controller allowing routing of thermal flows.

ABSTRAKT

Systematické řízení tepelných a elektrických toků v plně elektrických automobilech se stává velmi důležitým, protože v těchto typech automobilů není k dispozici dostatek odpadního tepla pro vytápění kabiny. Aby v zimním období nedocházelo ke snížení dojezdu, je nutné použití technologií, které umožní snížení spotřeby energie nutné k vytápění kabiny (např. tepelné čerpadlo, zásobník tepla). Je také zapotřebí vytvořit řídicí algoritmy pro tato zařízení, aby byl zajištěn jejich optimální provoz. V letním období je nezbytné řídit tepelné toky v rámci elektromobilu tak, aby nedocházelo k nadměrnému vybíjení baterie kvůli chlazení kabiny a dalších částí. Tato práce řeší jak návrh řídicích algoritmů, tak i vývoj rozhodovacího algoritmu, který zajistí směřování tepelných toků.